Thermo-Mechanical Fatigue of Cast 319 Aluminum Alloys

Huseyin Sehitoglu, [1] Carlos C. Engler-Pinto Jr. [2],
Hans J. Maier [3] ,Tracy J. Foglesong[4]

[1] University of Illinois at Urbana- Champaign, USA,
[2] Ford Motor Company, Dearborn, [3] Universität-GH Paderborn, Germany, [4] Exxon , Houston

Research Supported by Ford Motor Company

Outline

- Use of Aluminum Alloys in engine blocks and cylinder heads
- Thermo-Mechanical Fatigue Results
- Summary
- Modeling Studies (Precipitation hardened aluminum alloys)

Percentage of Vehicles with Aluminum Engine Blocks and Heads (*)

		1994	2000	2005
Heads				
	Passenger cars	78%	85%	95%
	Light trucks	20%	40%	60%
Blocks				
	Passenger cars	13%	30%	50%
	Light trucks	5%	10%	20%

(*) Delphi VIII Study, 1996

Advantages of cast aluminum

- Lightweight
  - V-8 Engine Block: 150 lbs Cast Iron vs. 68 lbs Aluminum
- Cast into complex shapes
- Increased thermal conductivity

Practical Application

- Cylinder Heads

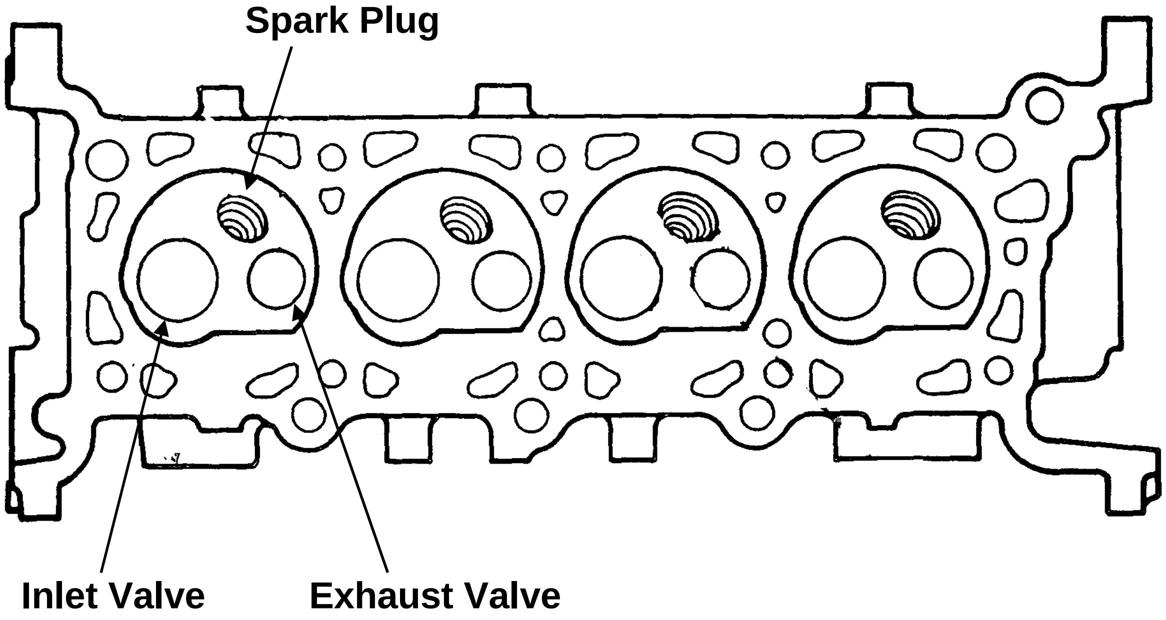

Al319-T7B

- Nominal Composition in weight percentage

Al	Si	Cu	Mg	Mn	Fe	Zn	Ti	Cr
Bal.	7.2-7.7	3.3-3.7	0.25-0.35	0.20-0.30	*	0.25 max	0.25 max	0.05 max

  - (*) WAP319: max 0.4% Fe - EAP319: max 0.8% Fe
- Thermal treatment
  - solutionizing at 495°C for 8 hours followed by precipitating at 260°C for 4 hours)

Thermo-Mechanical Fatigue Cycles

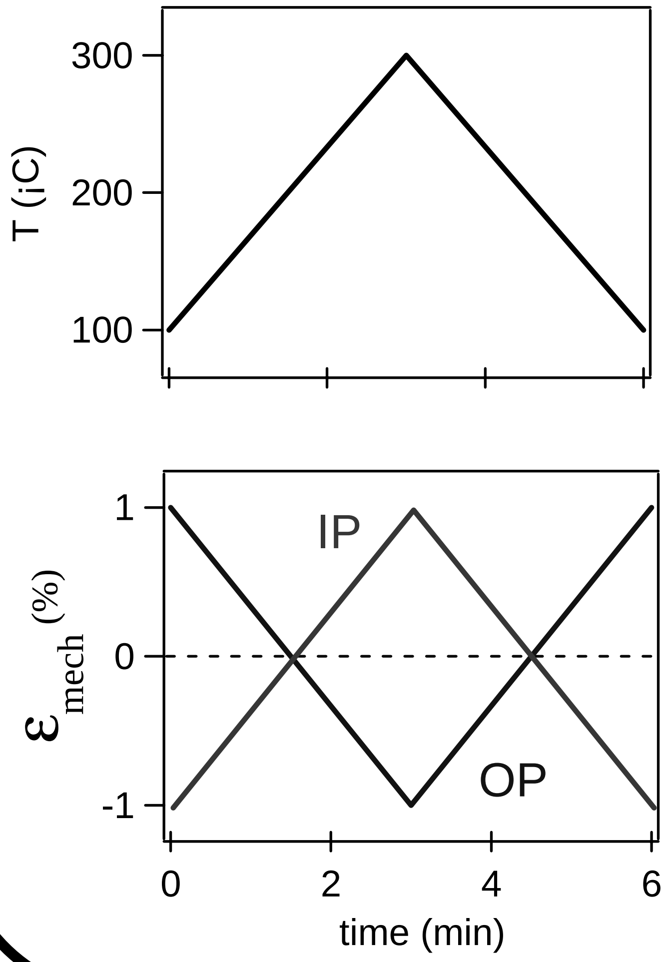

- Simultaneously changing strain and temperature (T)
- **In-Phase**: max-strain at max-T
- **Out-of-Phase**: max-strain at min-T

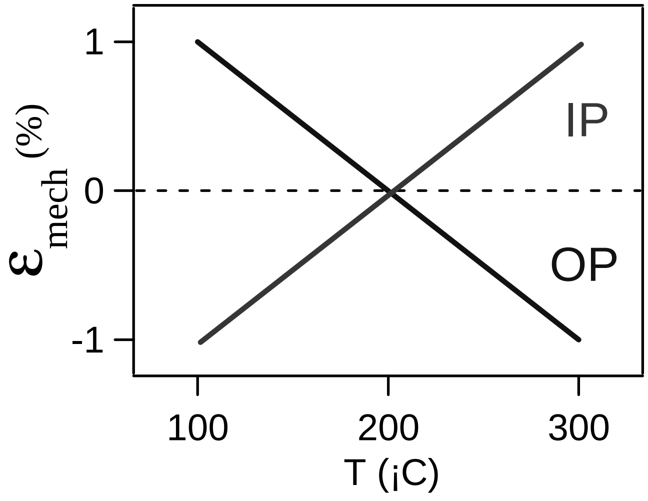

Thermo-Mechanical Fatigue

- Fatigue of materials subjected to simultaneously changing temperature and strain.

- $\varepsilon_{tot} = \varepsilon_{th} + \varepsilon_{mech}$

- Terminology
  - in-phase
  - out-of-phase

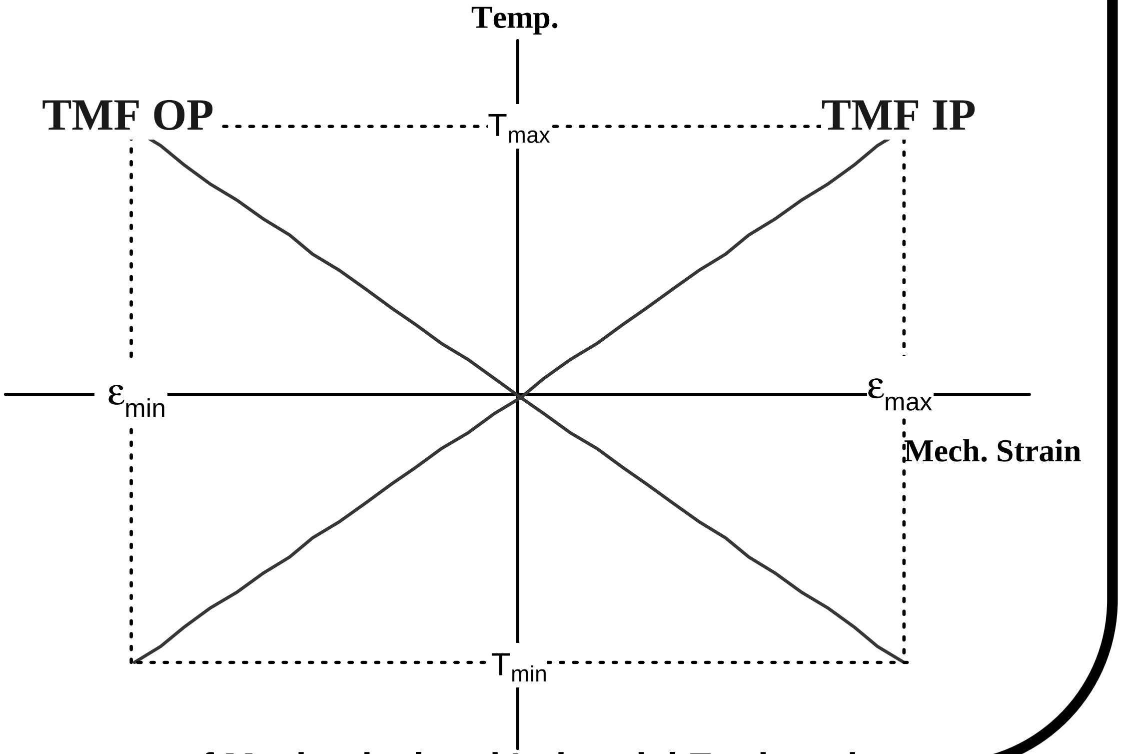

TMF Testing

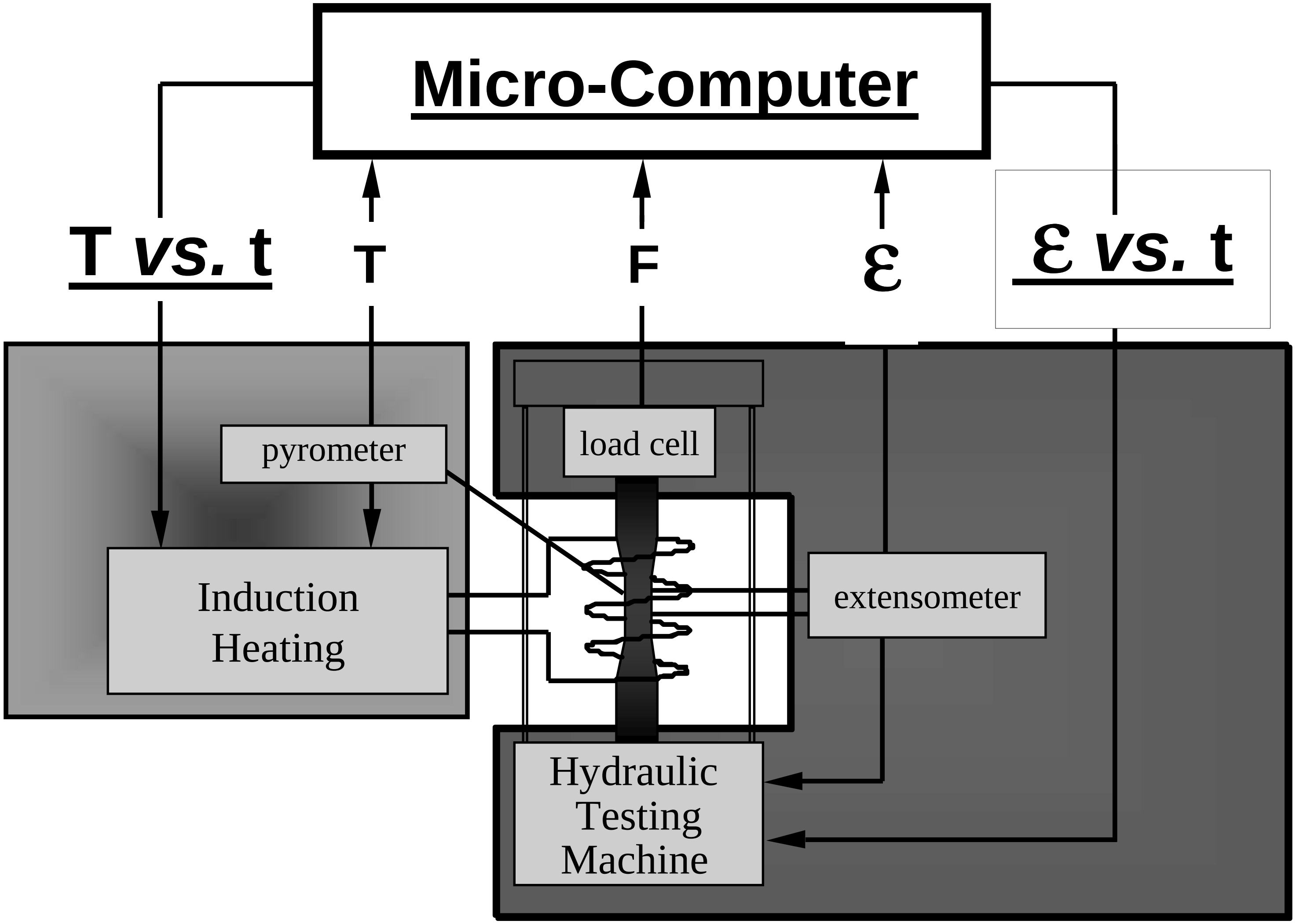
Micro-Computer
T vs. t
T
F
ε
ε vs. t
pyrometer
load cell
Induction Heating
extensometer
Hydraulic Testing Machine

Experimental Procedures

- Isothermal LCF
  - 20°C, 150°C, 250°C and 300°C
  - 2×10^{-1} s^{-1}, 4×10^{-3} s^{-1} and 5×10^{-5} s^{-1}
- Thermo-Mechanical Fatigue
  - 100–300°C — 5×10^{-5} s^{-1}

TMF Loops

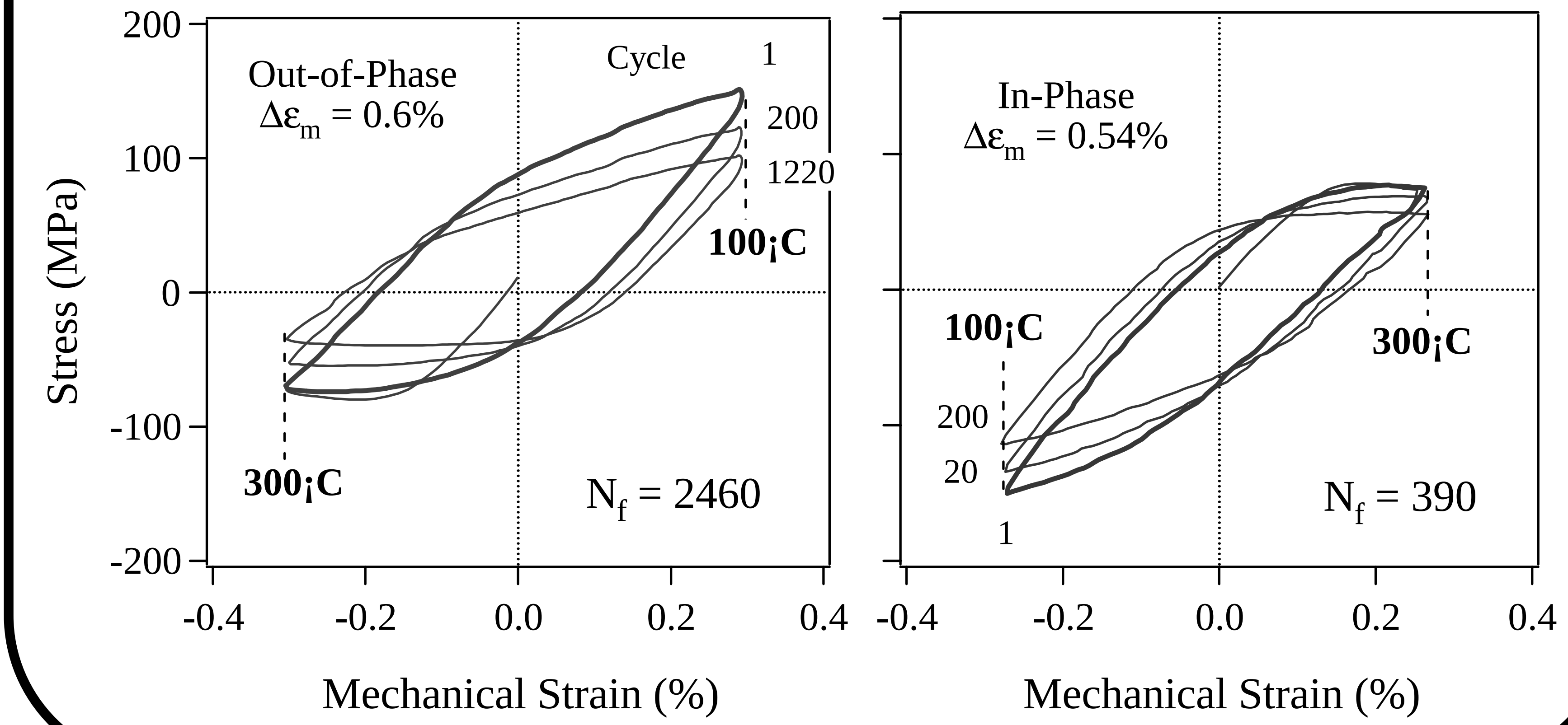
200
100
0
-100
-200
Stress (MPa)
Out-of-Phase
$\Delta\varepsilon_m$ = 0.6%
Cycle
1
200
1220
100¡C
300¡C
N_f = 2460
-0.4
-0.2
0.0
0.2
0.4
Mechanical Strain (%)
In-Phase
$\Delta\varepsilon_m$ = 0.54%
100¡C
300¡C
200
20
1
N_f = 390
-0.4
-0.2
0.0
0.2
0.4
Mechanical Strain (%)

TMF OP 100-300°C 1.0%

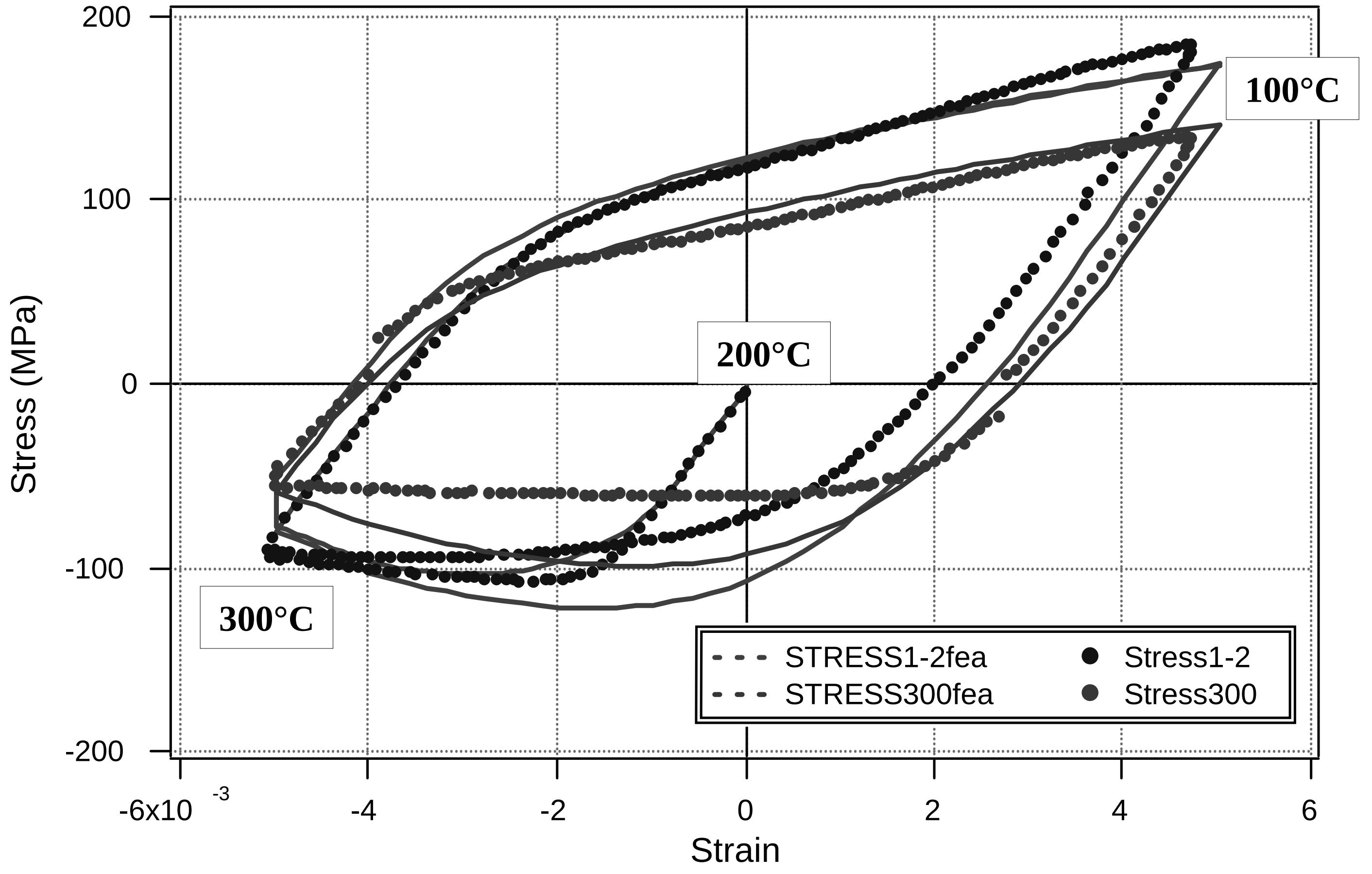

Fatigue Life Criterion

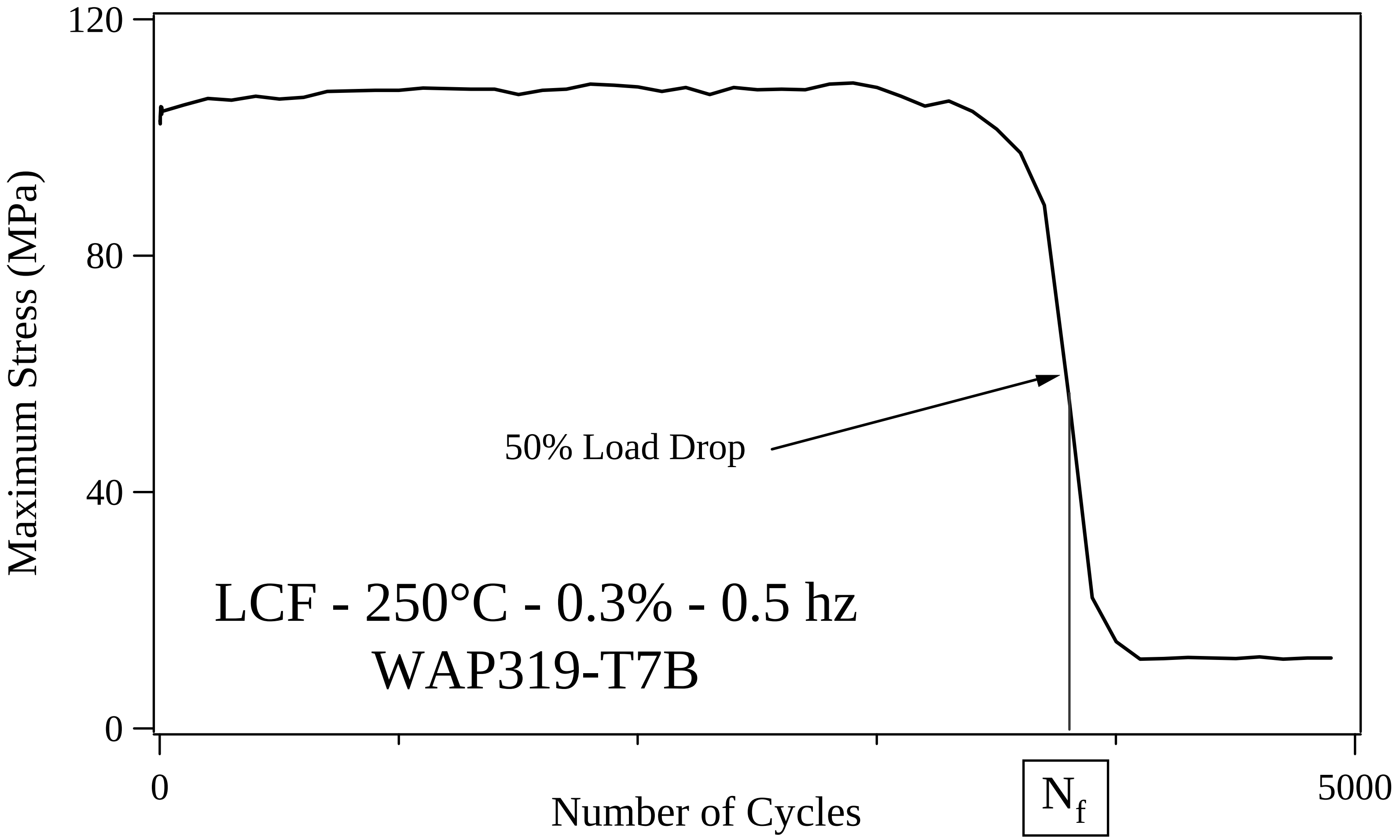

Precipitate Coarsening

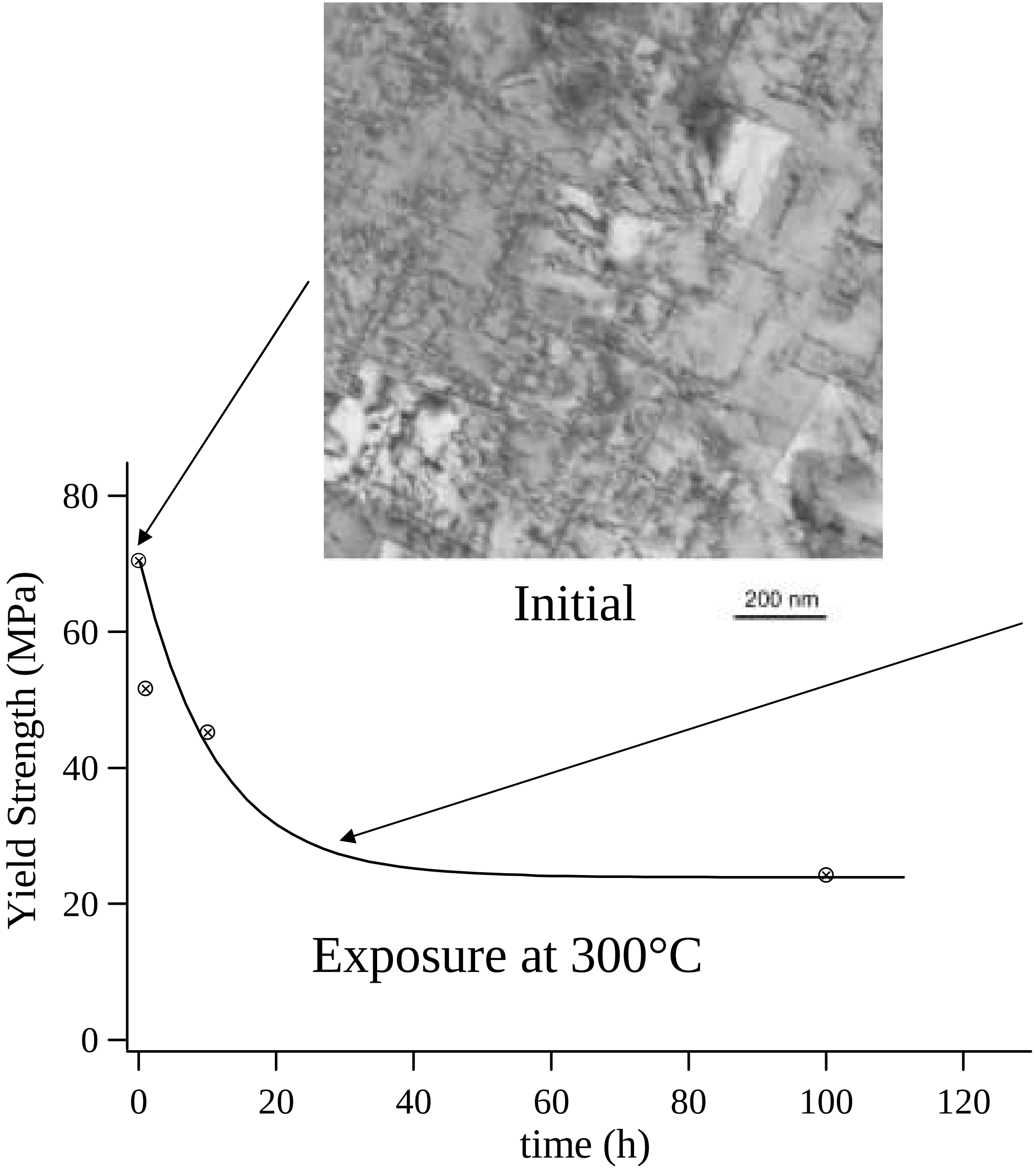

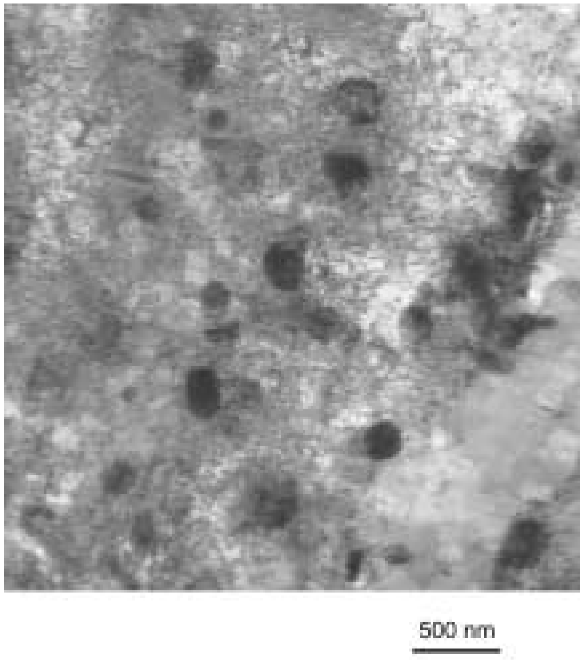

45000 cycles / ~25 hours (300°C, $\Delta\varepsilon_m = 0.2\%$).

TMF Loops

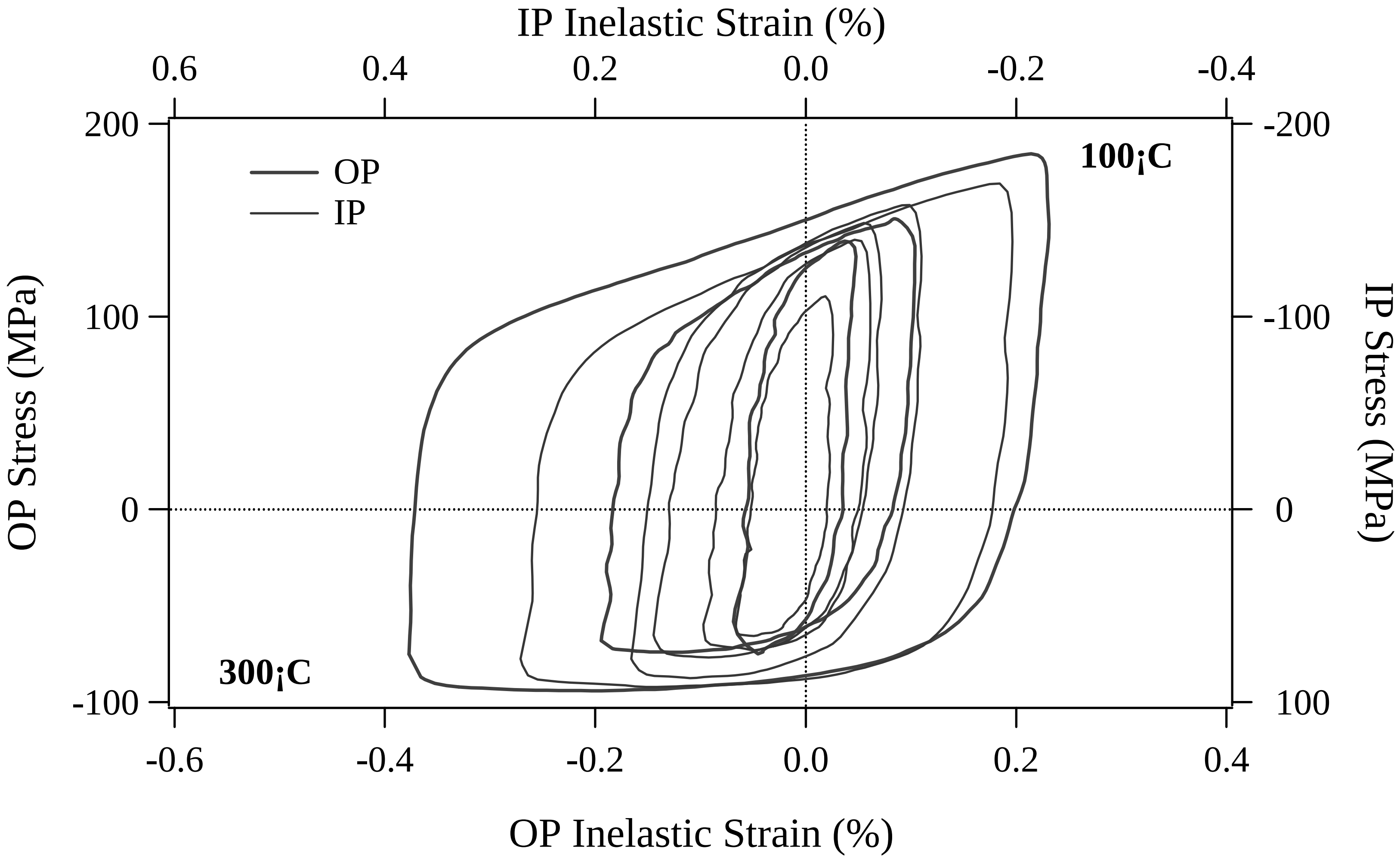
IP Inelastic Strain (%)
0.6
0.4
0.2
0.0
-0.2
-0.4
200
100
0
-100
-200
-100
0
100
OP
IP
100¡C
300¡C
OP Stress (MPa)
IP Stress (MPa)
-0.6
-0.4
-0.2
0.0
0.2
0.4
OP Inelastic Strain (%)

TMF – Peak Stresses

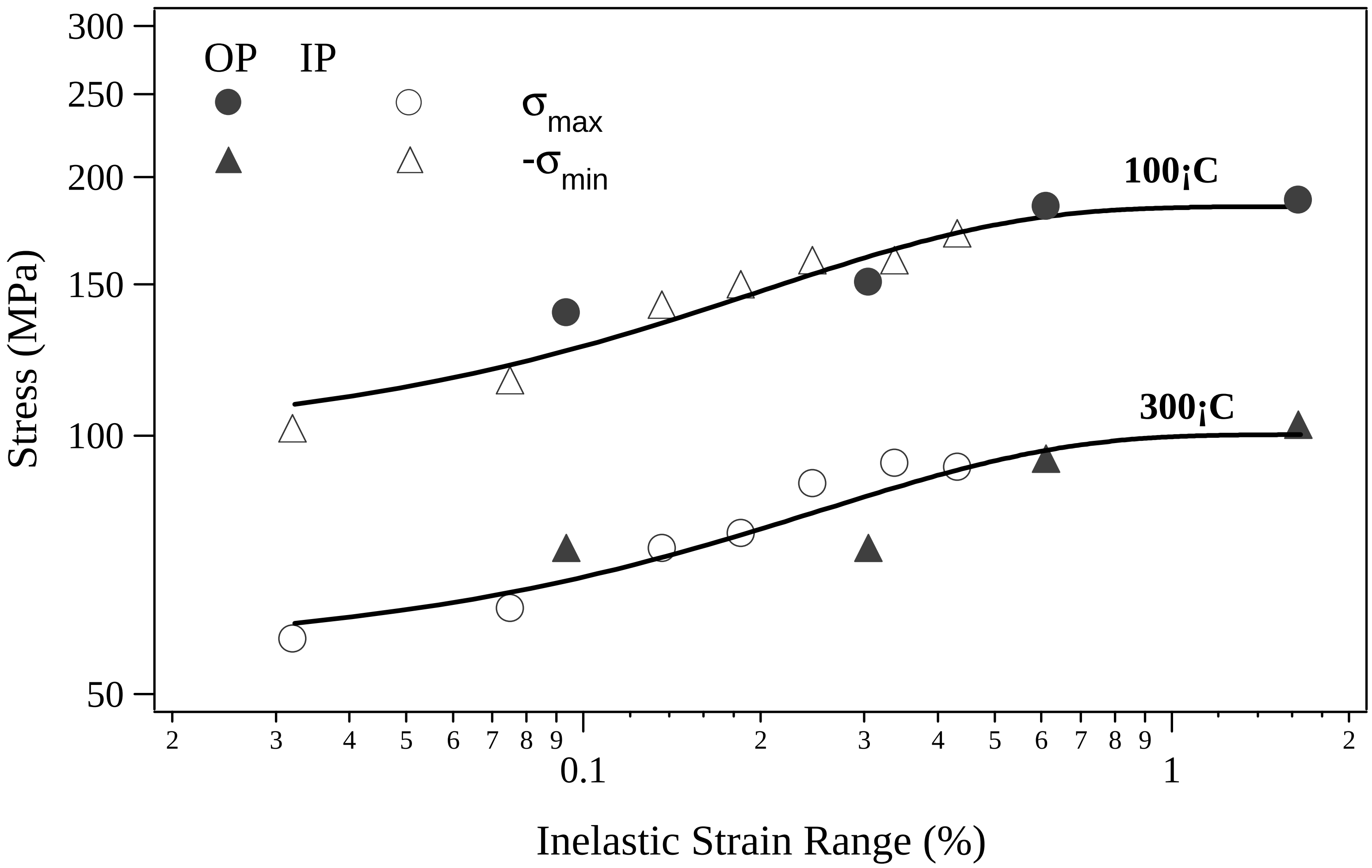

TMF – Stress Range Evolution

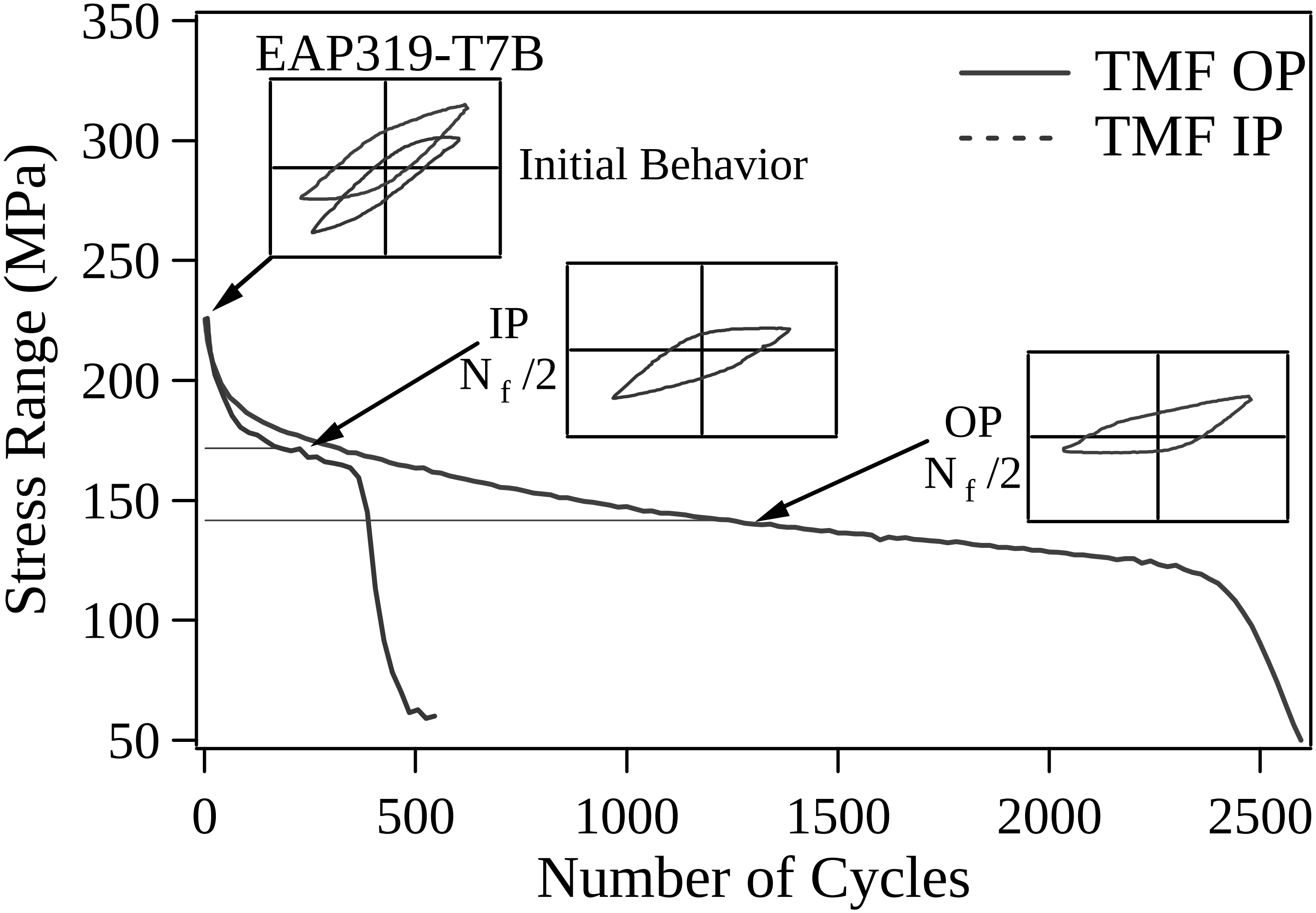

Cyclic Stress-Strain Curves

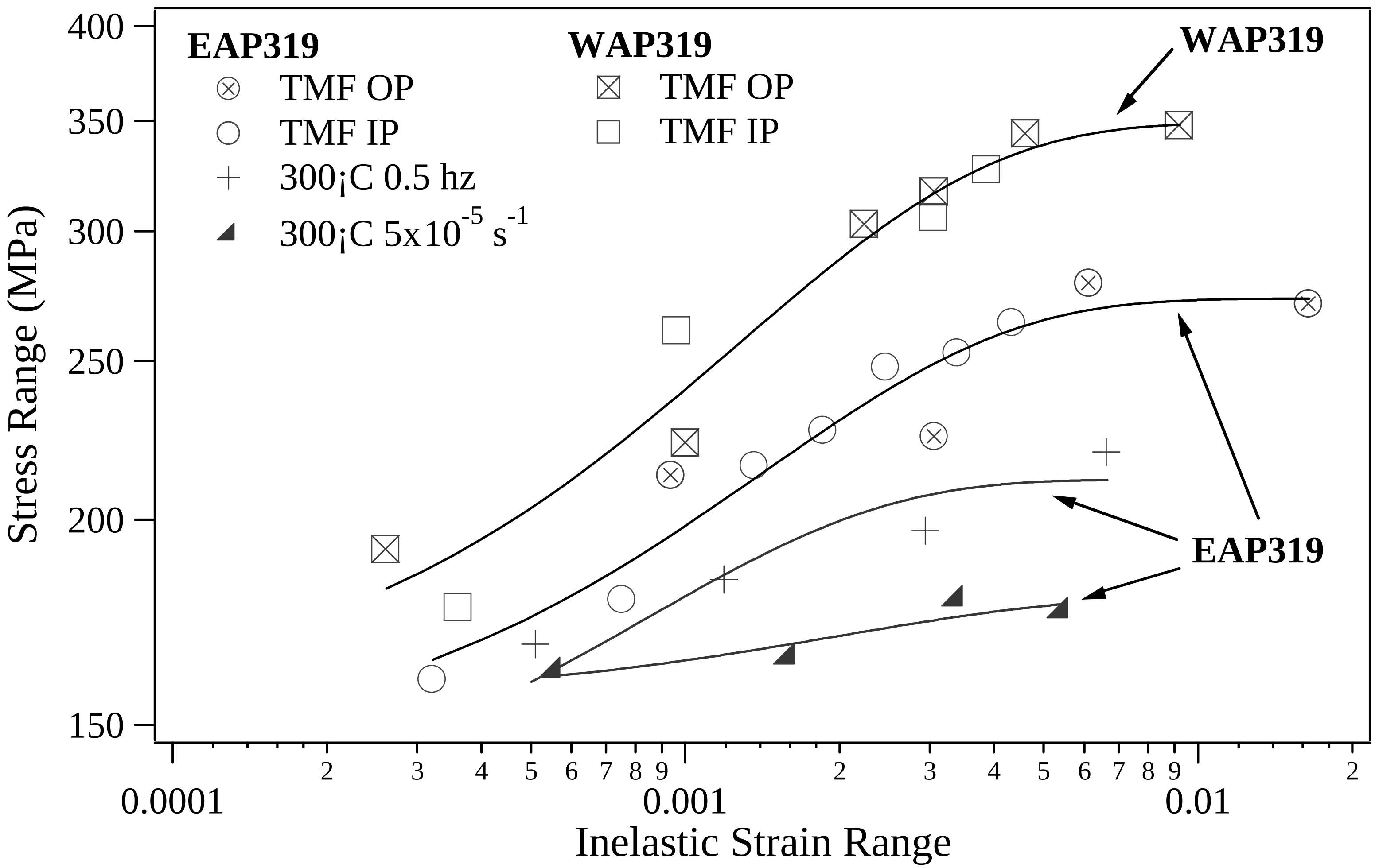

TMF Life

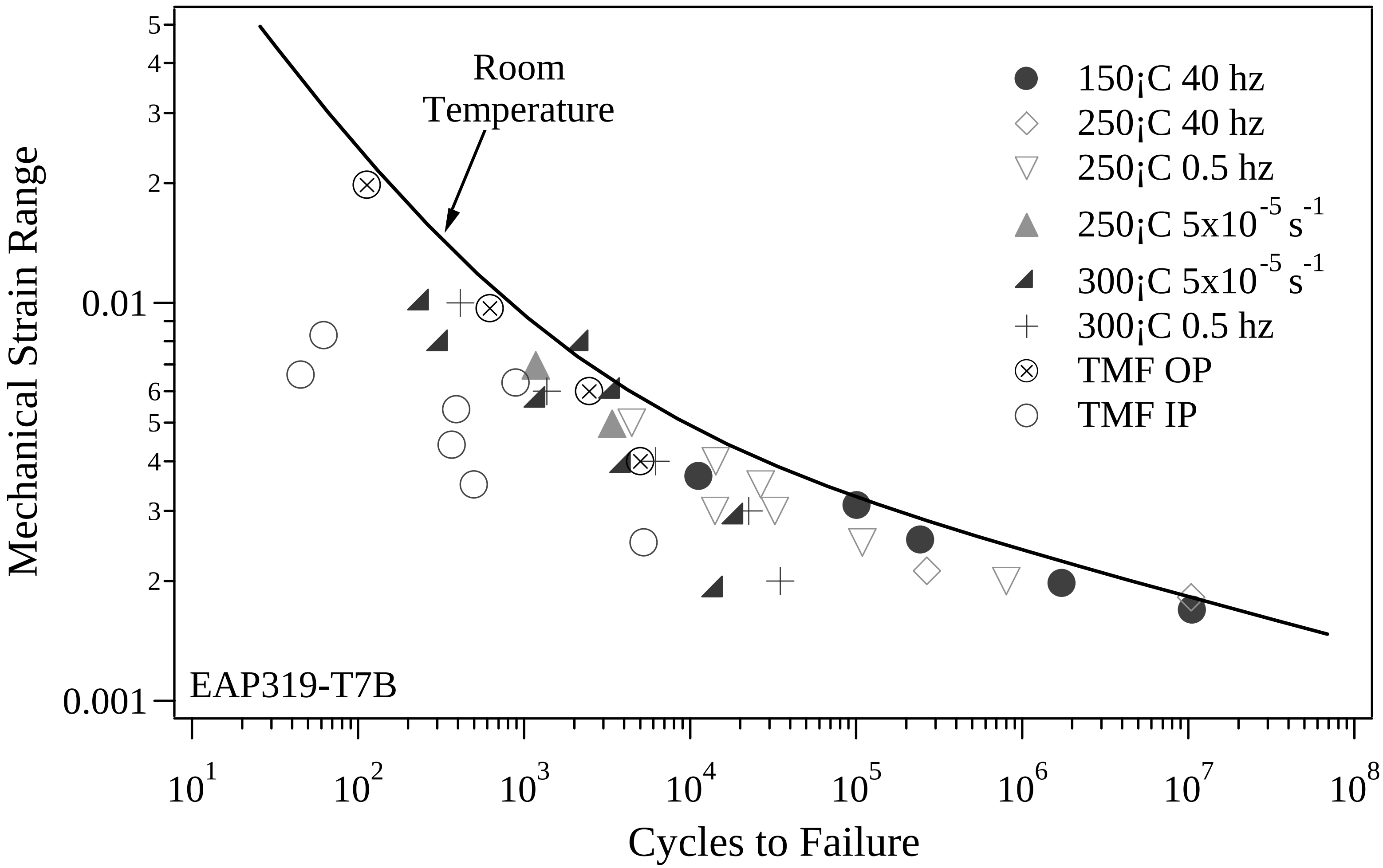
Room Temperature
● 150¡C 40 hz
◇ 250¡C 40 hz
▽ 250¡C 0.5 hz
▲ 250¡C 5x10^{-5} s^{-1}
◢ 300¡C 5x10^{-5} s^{-1}
+ 300¡C 0.5 hz
⊗ TMF OP
○ TMF IP
EAP319-T7B
Mechanical Strain Range
5
4
3
2
0.01
6
5
4
3
2
0.001
10^1
10^2
10^3
10^4
10^5
10^6
10^7
10^8
Cycles to Failure

TMF Life

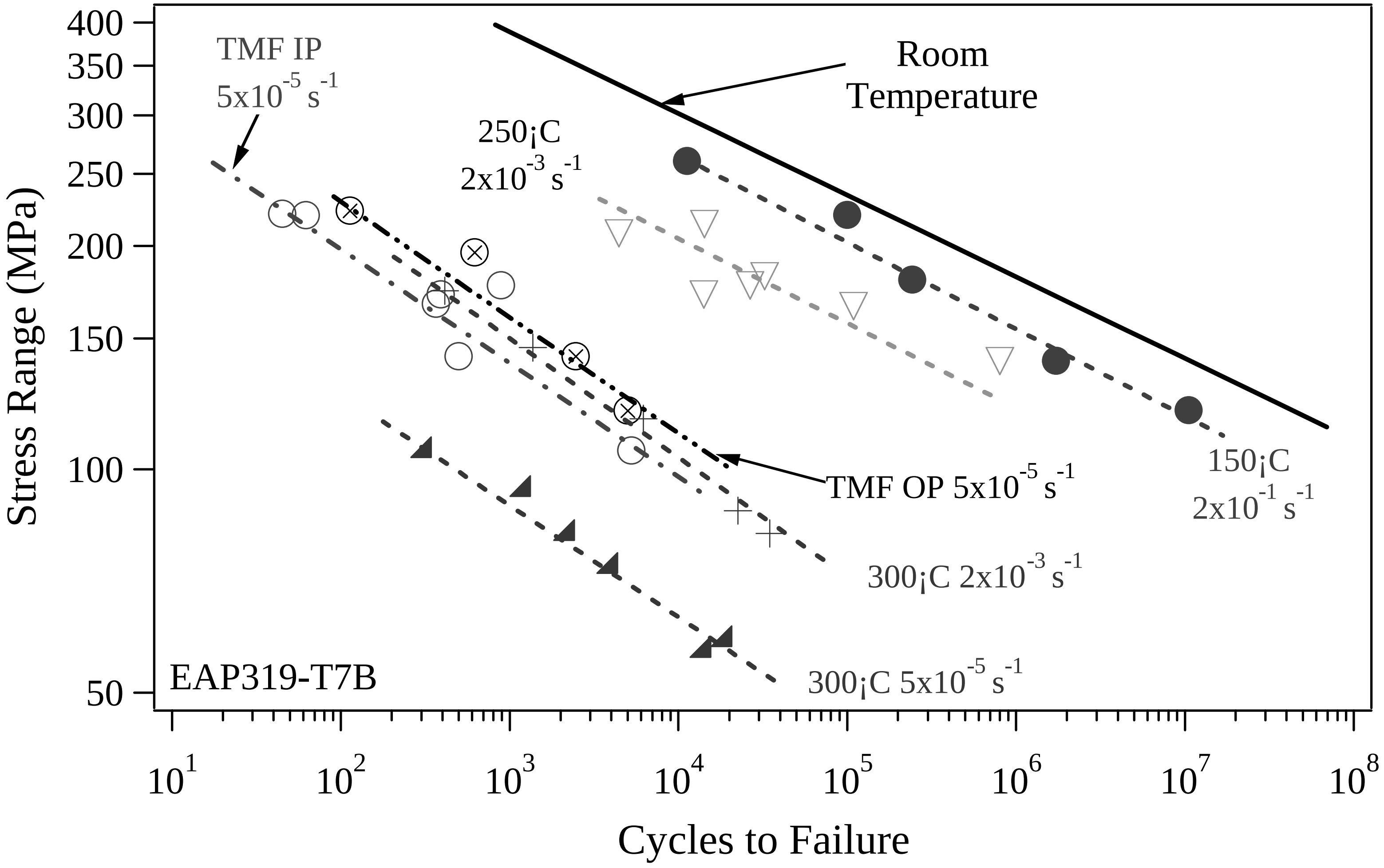
TMF IP
5x10^{-5} s^{-1}
Room
Temperature
250¡C
2x10^{-3} s^{-1}
TMF OP 5x10^{-5} s^{-1}
150¡C
2x10^{-1} s^{-1}
300¡C 2x10^{-3} s^{-1}
300¡C 5x10^{-5} s^{-1}
EAP319-T7B
Stress Range (MPa)
400
350
300
250
200
150
100
50
10^1
10^2
10^3
10^4
10^5
10^6
10^7
10^8
Cycles to Failure

TMF Life

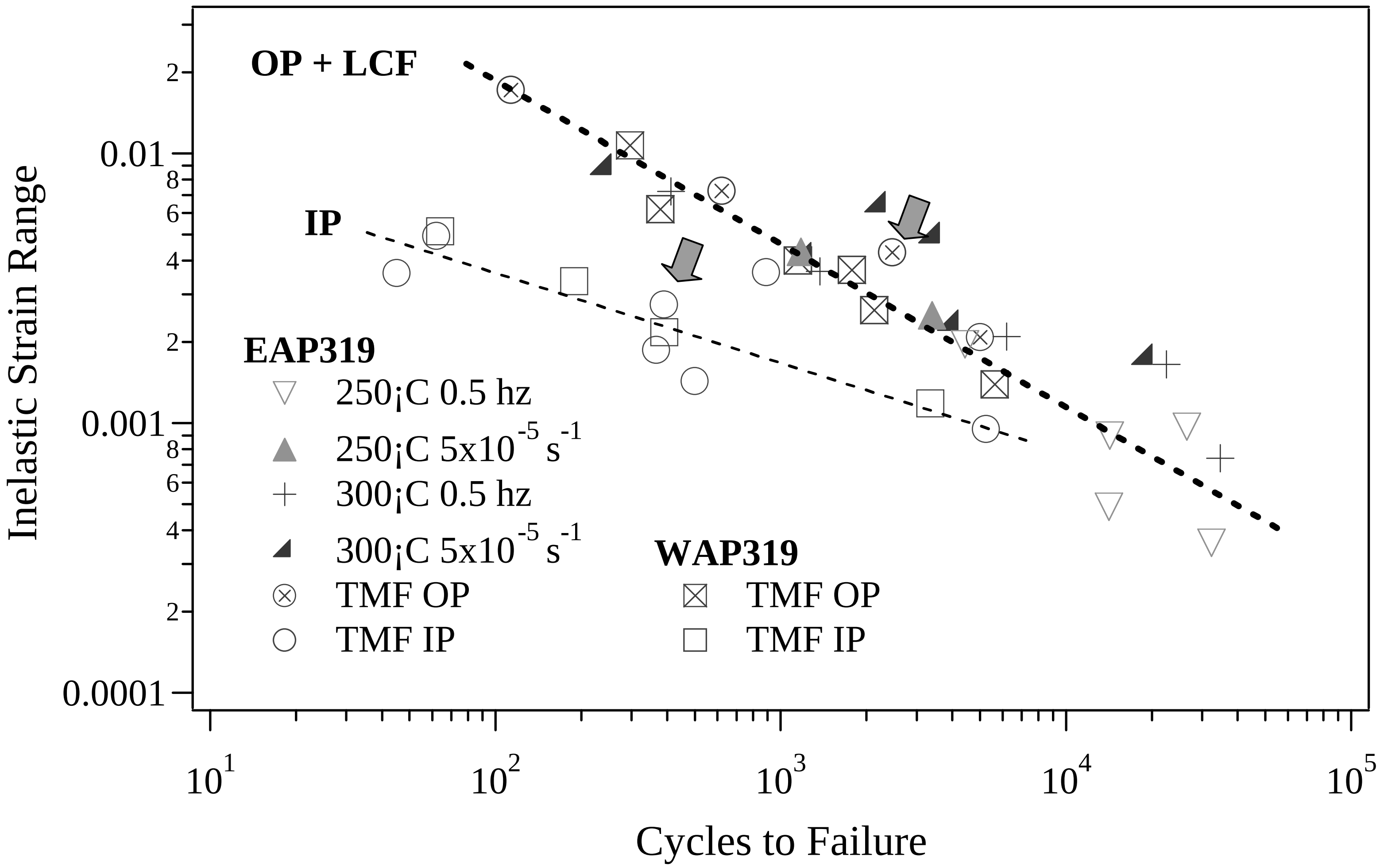
OP + LCF
IP
Inelastic Strain Range
0.0001
2
4
6
8
0.001
2
4
6
8
0.01
2
10^1
10^2
10^3
10^4
10^5
Cycles to Failure
EAP319
▽ 250¡C 0.5 hz
▲ 250¡C 5x10^{-5} s^{-1}
+ 300¡C 0.5 hz
◢ 300¡C 5x10^{-5} s^{-1}
⊗ TMF OP
○ TMF IP
WAP319
⊠ TMF OP
□ TMF IP

EAP319-T7B

TMF-OP

100–300°C

$\Delta\varepsilon_m$=0.6%

N_f=2460 c.

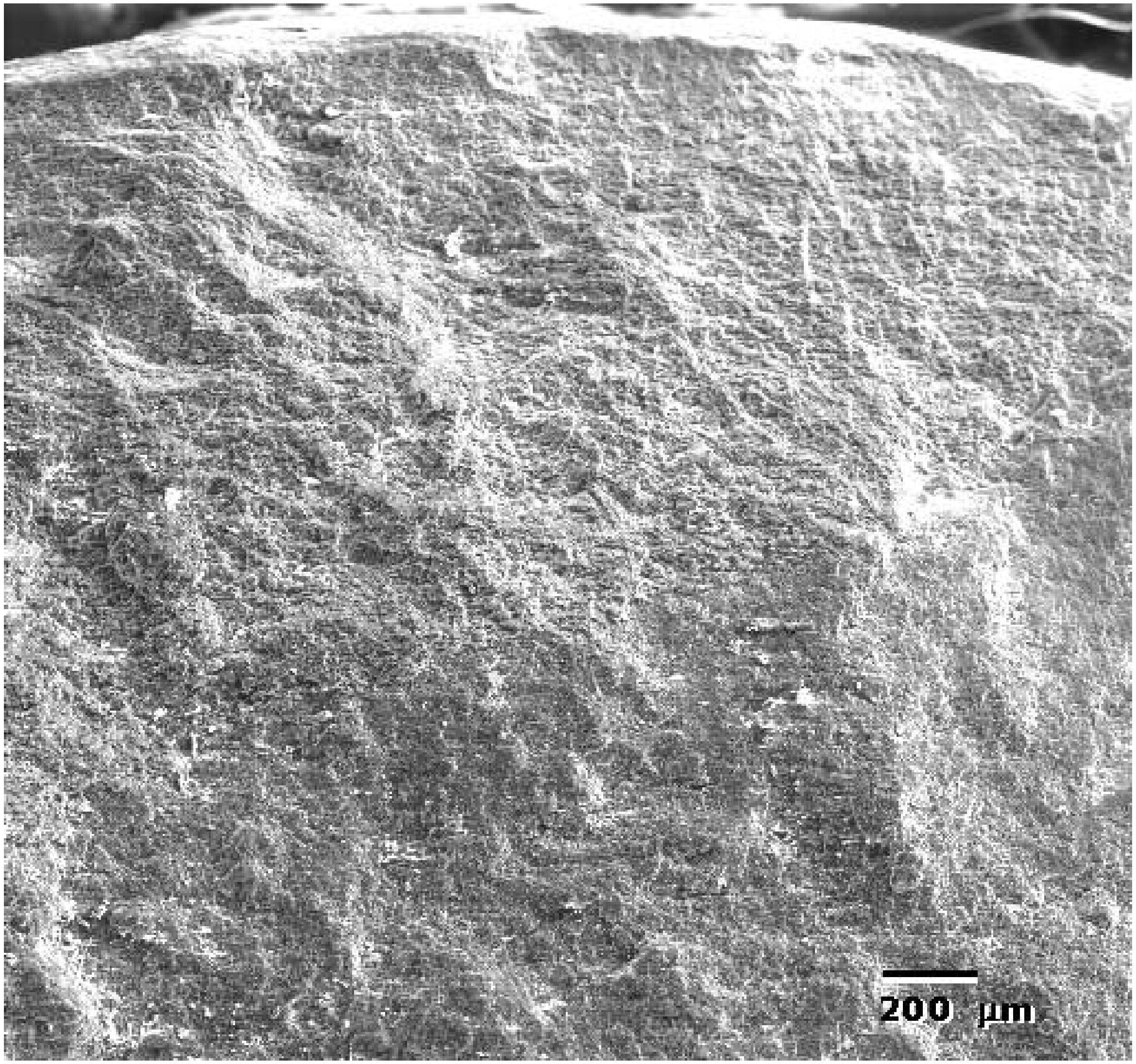

EAP319-T7B

TMF-IP

100–300°C

$\Delta\varepsilon_m$=0.54%

N_f=390 c.

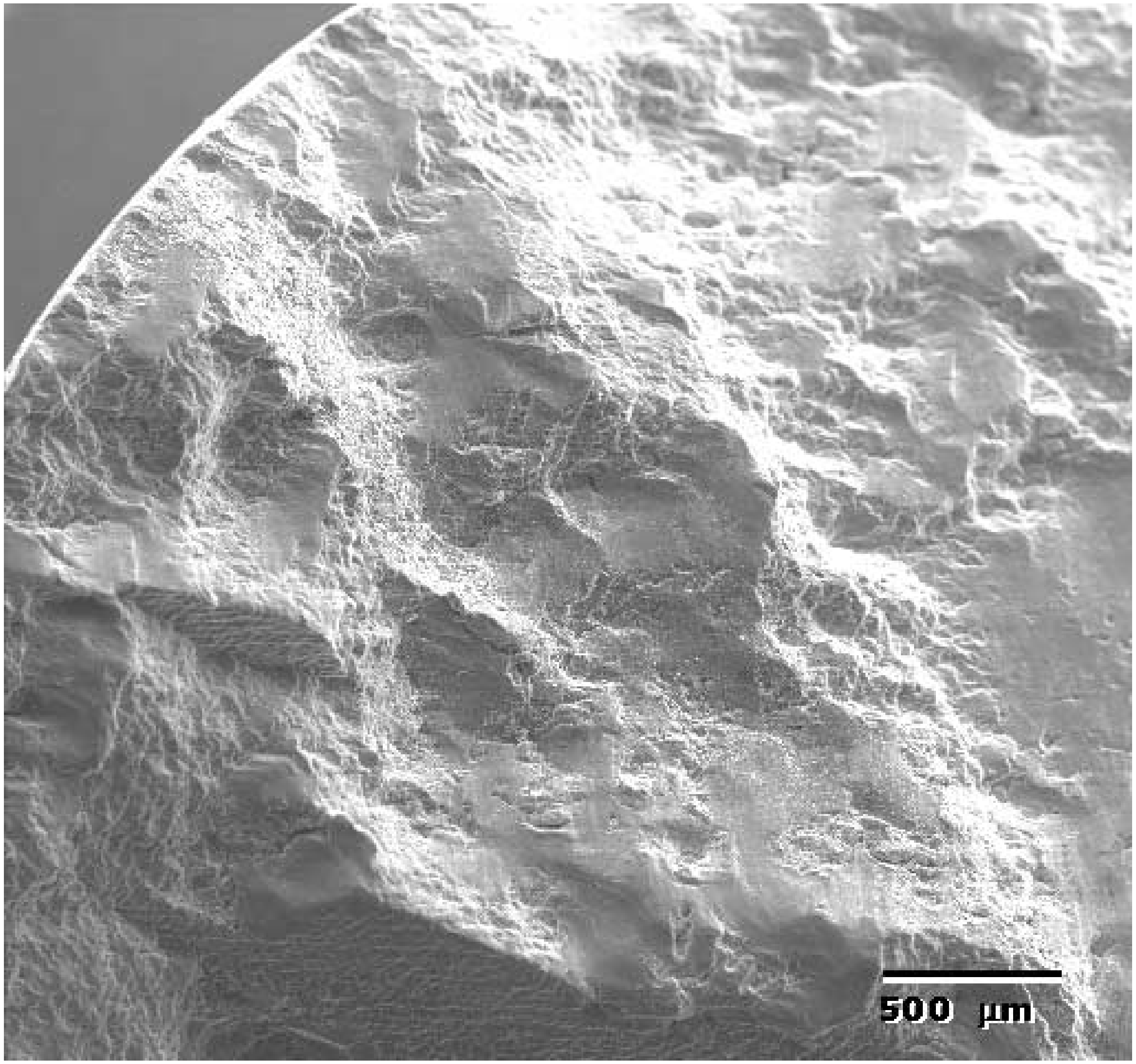

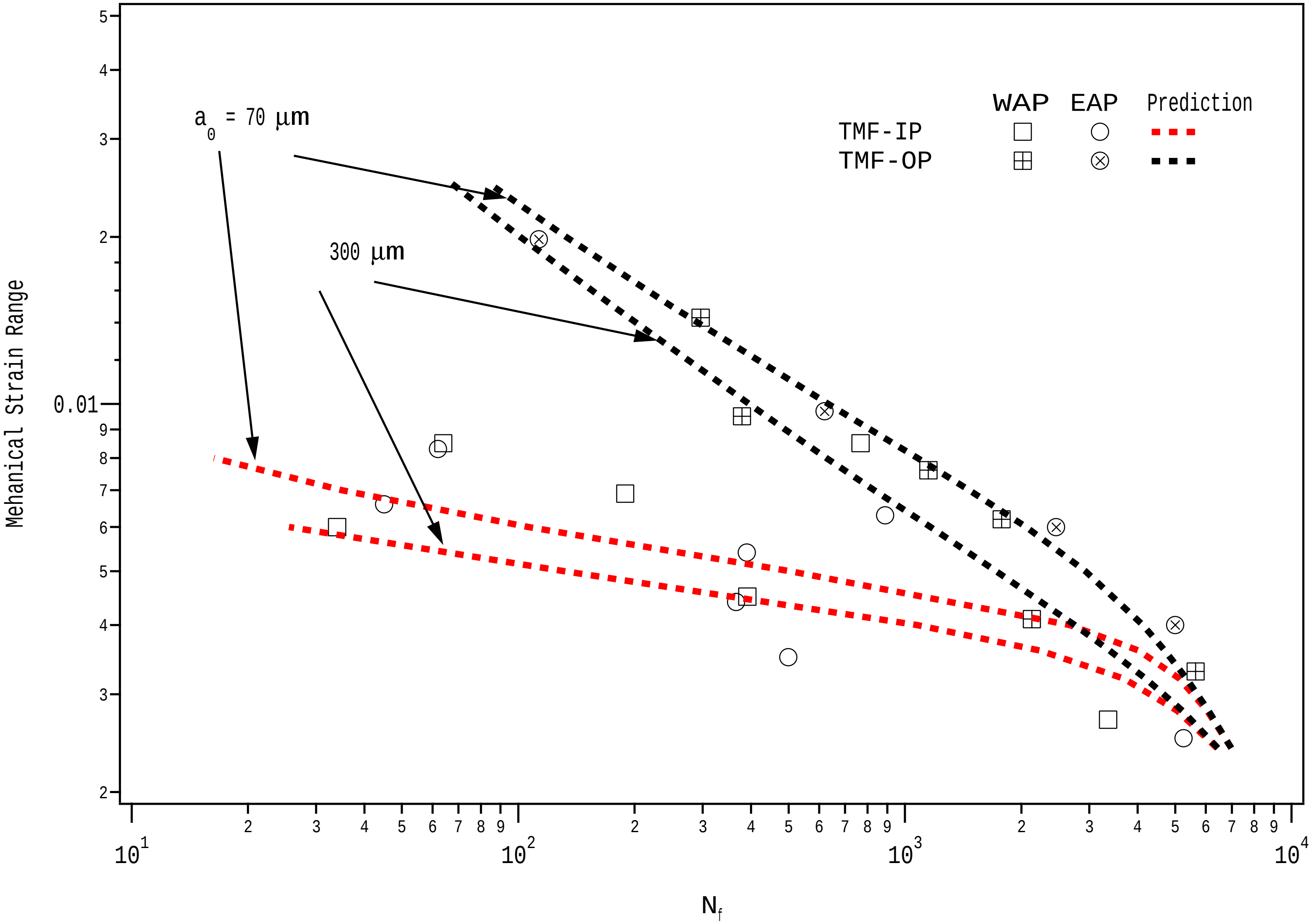
Mehanical Strain Range
0.01
2
3
4
5
6
7
8
9
N_f
10^1
10^2
10^3
10^4
a_0 = 70 µm
300 µm
WAP
EAP
Prediction
TMF-IP □ ○
TMF-OP ⊞ ⊗

Summary

1. TMF stress-strain behavior is identical for both IP and OP loading conditions. TMF-IP lives are shorter than TMF-OP (based on the mechanical or inelastic strain range) lives.

2. Creep damage dominates for TMF-IP loading and in the high strain range regime.

3. The secondary alloy (EAP319) is softer than the primary alloy (WAP319), but TMF lives are very similar.

Aluminum-Copper Alloys

- Precipitate-dislocation interactions
  - Anisotropy on plastic flow behavior (Hosford & Zeisloft ‘72, Bate *et al.* ‘81, Barlat & Liu ‘98, Choi & Barlat ‘99)
  - Bauschinger effect (Abel & Ham ‘66, Moan & Embury ‘79, Wilson ‘65)
- Coherent particles - GP zones and θ'' (Price and Kelly ‘64)
  - Higher yield stress than Al shearing of particles
  - Comparable work hardening rates and deformation to Al
- Semi-coherent - θ' (P & K ‘64, Russell & Ashby ‘70)
  - High yield stress and high work hardening rates
- Incoherent particles - θ (P & K ‘64, R & A ‘70)
  - Low initial yield stress
  - Highest rates of work hardening

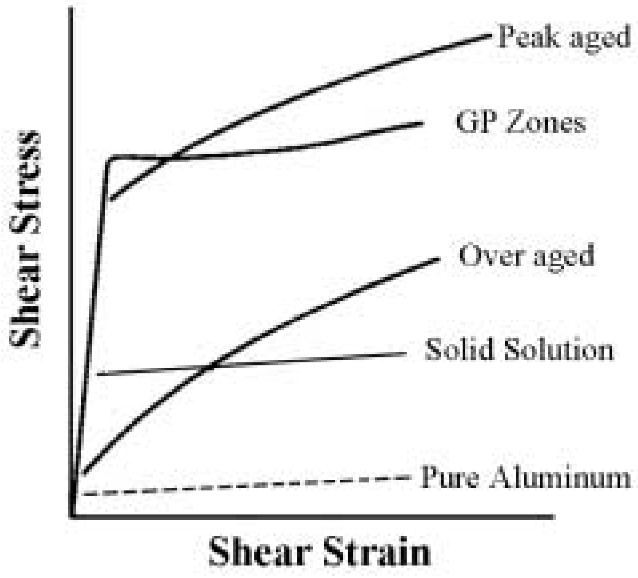

Precipitate Development

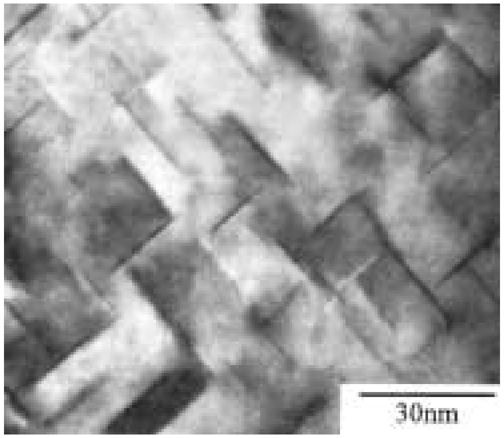

GP zones *

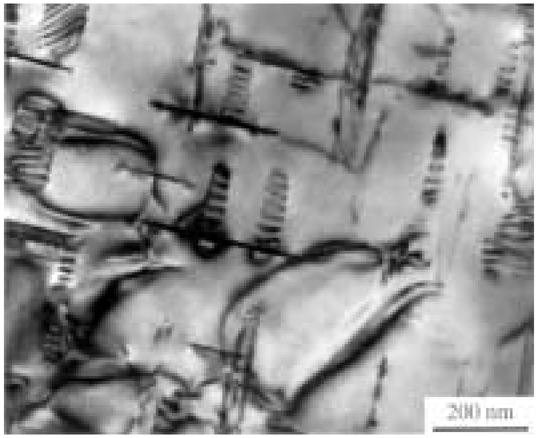

Peak aged, θ'

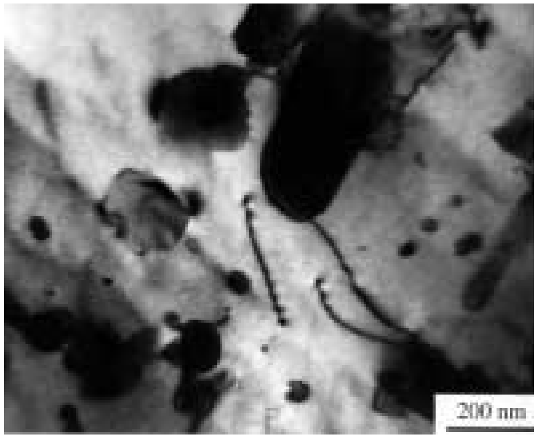

Very over aged, coarse θ

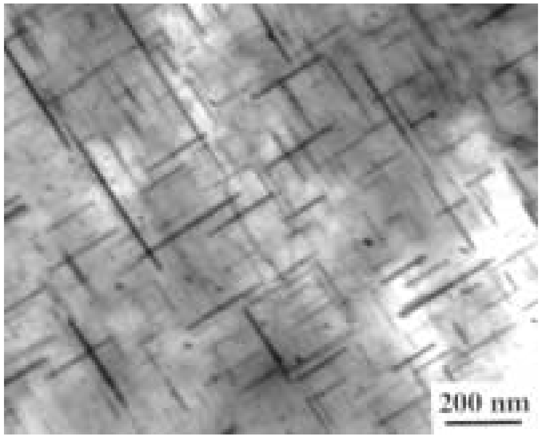

Over aged, θ' & fine θ

*Sato & Takahashi, 1983

Limitations of current models

- No implicit consideration of aging treatment.
  - Models were developed for one specific aging treatment
    - Peak aged, θ'
- No inclusion of length scale
  - Volume fraction, precipitate size, mean free path etc. with aging treatment
- Empirical hardening models with a microstructural basis.

Proposed Hardening Law

- Single crystal formulation - one precipitate type

$$\dot{\tau} = \left[\frac{K_o\alpha^2\mu^2 b}{2(\tau-\tau_o)d} + \theta_o\left(\frac{\tau_s-\tau}{\tau_s-\tau_o}\right)\right]\sum_k\left|\dot{\gamma}^k\right|$$

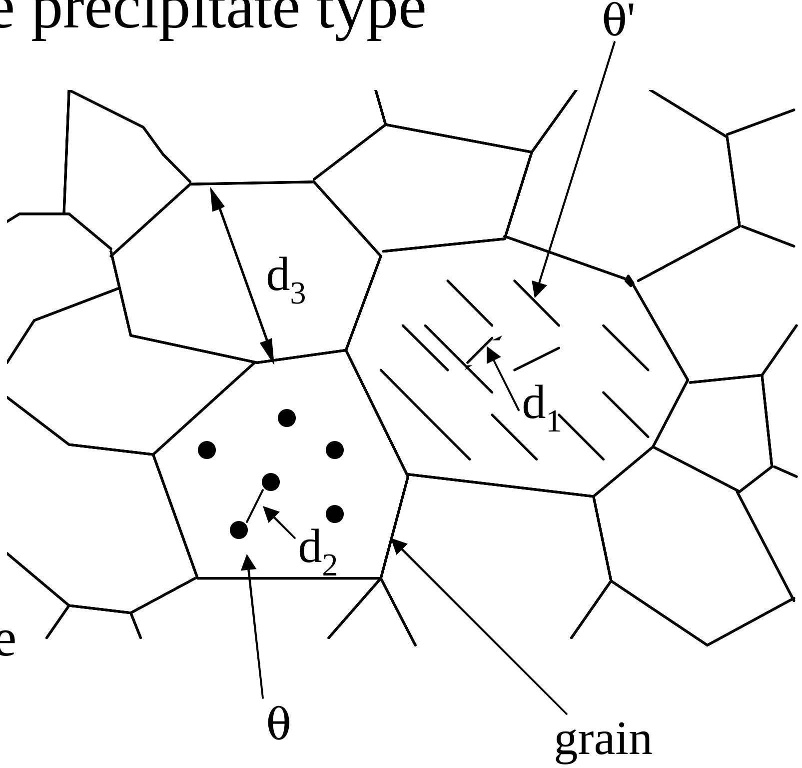

- Polycrystal formulation
  - More than one type of precipitate
  - Incorporate grain size length scale

$$\dot{\tau} = \left[\frac{\mu^2 b}{2(\tau-\tau_o)}\left(\frac{\alpha_1^2K_1'}{d_1}+\frac{\alpha_2^2K_2'}{d_2}+\frac{\alpha_3^2K_3'}{d_3}\right) + \theta_o\left(\frac{\tau_s-\tau}{\tau_s-\tau_{o3}}\right)\right]\sum_k\left|\dot{\gamma}^k\right|$$

Constitutive Equations

- Relate stress and strain rate at single crystal and polycrystal level.

$$\dot{\varepsilon}_i^{in} = \left\{ \dot{\gamma}^0 \sum_{s=1}^{S} \frac{m_i^s m_j^s}{\tau_c^s} \left(\frac{m_k^s \sigma'_k}{\tau_c^s} \right)^{n-1} \right\} \sigma'_{\mathrm{j}} \qquad \text{where } i = 1,5$$

- Can be written in pseudo-linear form.

$$\boxed{\dot{\varepsilon}_i^{in} = M_{ij}^{c(\mathrm{sec})}(\sigma')\sigma'_j}$$

- Assume overall polycrystal response described by law similar to that of single crystal.

$$\boxed{\dot{E}_i^{in} = M_{ij}^{(\mathrm{sec})}(\bar{\Sigma}')\bar{\Sigma}'_j}$$

Hardening with Precipitates

- Start with dislocation evolution equation

$$\dot{\rho} = \sum_k \left[\frac{K_o}{db} + k_1\sqrt{\rho} - k_2\rho \right] \left|\dot{\gamma}_k\right|$$

Geometric storage term due
to boundaries / obstacles

Dynamic recovery
of dislocations

Statistical storage of dislocations

- Combine with the Bailey-Hirsch relationship for flow stress.

$$\tau = \tau_o + \alpha\mu b\sqrt{\rho}$$

Experiment and Simulation for Al - 4% Cu Single Crystals [123] Orientation - Different Aging Conditions

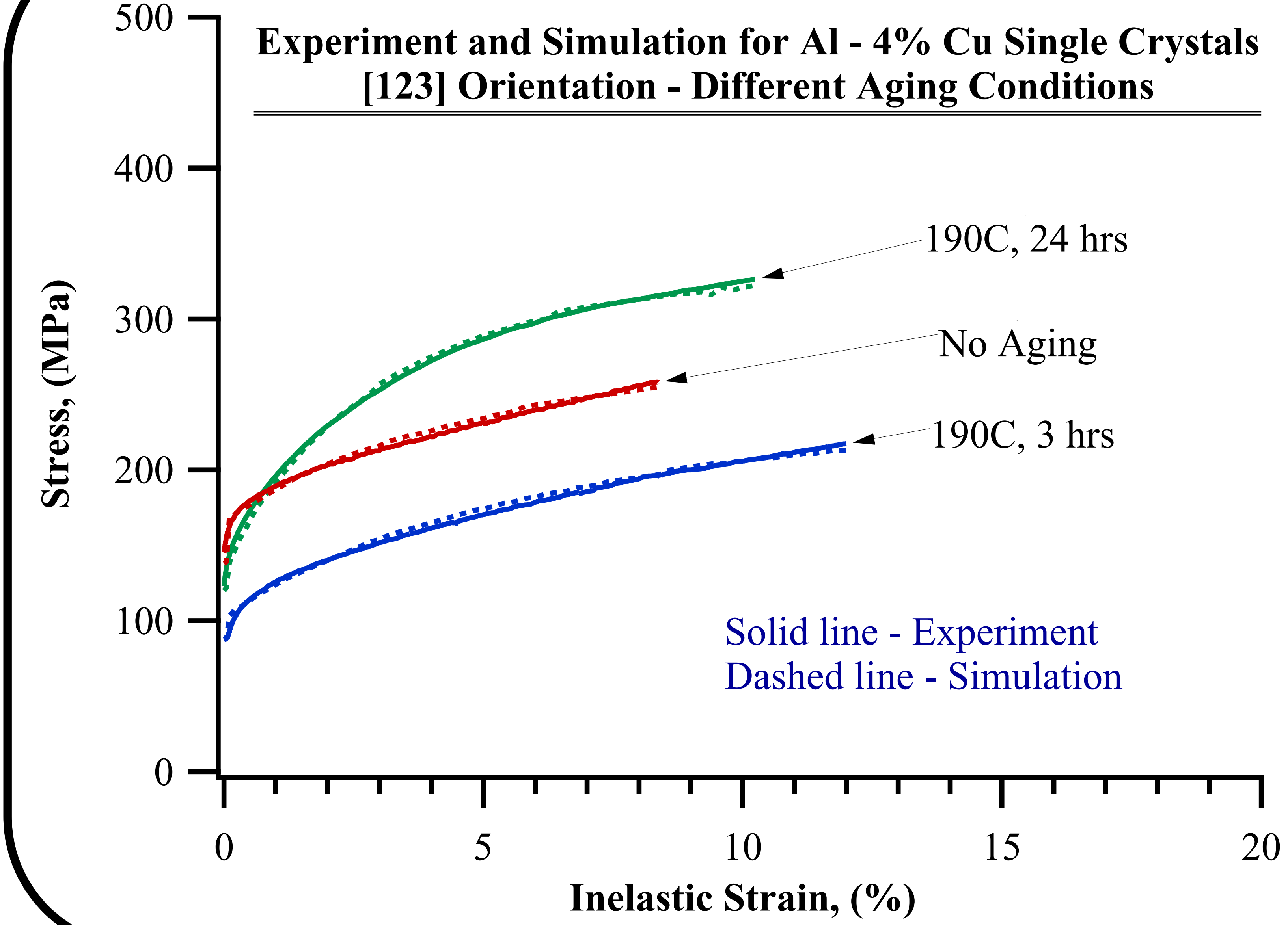

Summary

- The hardening law including the effects of precipitates on the deformation behavior of binary Al - Cu alloys is physically based and accounts for precipitate size, orientation, and mean free path.
- The model incorporates hardening law and predicts single crystal behavior of pure Al and Al-Cu alloys, it also predicts polycrystalline experiments from knowledge of single crystal behavior.